ELSEVIER

Coordination Chemistry Reviews
151 (1996) 125–143

COORDINATION CHEMISTRY REVIEWS

Synthesis, structure and magnetic properties of ferritin cores with varying composition and degrees of structural order: models for iron oxide deposits in iron-overload diseases[1]

T.G. St. Pierre [a,2], P. Chan [a], K.R. Bauchspiess [a], J. Webb [a], S. Betteridge [b], S. Walton [b], D.P.E. Dickson [b]

[a] *School of Mathematical and Physical Sciences, Murdoch University, Perth, WA 6150, Australia*
[b] *Department of Physics, University of Liverpool, Liverpool L69 3BX, UK*

Contents

Abstract

The cage-like protein ferritin was used to form nanoscale iron-containing mineral particles in vitro with different structures and compositions by reconstituting the metal-free protein (apoferritin) with iron at different temperatures and in the presence of different quantities of phosphate. The products of reconstitution were studied with inductively coupled plasma

[1] Keynote lecture presented at the Third International Symposium on Applied Bioinorganic Chemistry (ISABC-3), Fremantle, Perth, Western Australia, 11–15 December 1994.

[2] Present address: Department of Physics, The University of Western Australia, Nedlands, WA 6907, Australia.

SSDI 0010-8545(95)01220-6

spectrometry, transmission electron microscopy, electron diffraction, extended X-ray absorption fine structure analysis, and Mössbauer spectroscopy. Reconstitution at 4 °C resulted in poorly ordered core structures while reconstitution at 55 °C resulted in more ordered structures based on that of the mineral ferrihydrite. The more ordered structure of the 55 °C ferritin resulted in stronger magnetic exchange interactions between the iron atoms within each core and a larger magnetic anisotropy energy per core. Incorporation of phosphate within the core structure reduced the core density. This also reduced the strength of the magnetic exchange interactions between the iron atoms. High levels of phosphate within the core resulted in cores with no measurable periodicity within their structure. This in turn caused a reduction in the magnetic anisotropy energy per core. The ability to tailor the degree of structural order and phosphate content of ferritin cores in vitro makes available a range of model materials for a more comprehensive study of the structural and magnetic correlations found in nanoscale iron biominerals in vivo such as native ferritins and haemosiderins deposited in iron-overloaded tissues.

Keywords: Ferritin; Biomineralization; Mössbauer spectroscopy; EXAFS

1. Introduction

Ferritin is a protein that consists of 24 subunits that are assembled to form a near-spherical cage-like structure. The external diameter is approximately 12 nm while the diameter of the cavity is about 8 nm. Channels connect the external space with the internal cavity such that ions may pass into and out from the central cavity [1]. Groups on the internal surface of the protein act as binding sites for iron and aid in the nucleation of inorganic iron(III) oxyhydroxide particles. Once nucleated, particles can continue to grow until the dimensions of the cavity restrict further growth. Ferritins isolated from mammalian tissue are usually found to contain particles of iron(III) oxyhydroxide with varying quantities of inorganic phosphate bound to/within the particle.

In mammals, ferritin is mainly involved in iron storage and homeostasis. Its capacity to store several thousand iron atoms per molecule (usually up to 4000 Fe/molecule) makes it ideally suited to this function. It is mainly found in the liver and spleen, the principal iron storage sites in the body. Under normal conditions ferritin is the site of deposition of any excess of iron [2]. However, in the case of iron-overload diseases such as haemochromatosis and thalassaemia where there is a much greater excess, iron is found deposited as various forms of iron(III) oxyhydroxide that are not associated with the protein ferritin. These forms are collectively known as haemosiderin. Like ferritin, the iron mineral components of haemosiderin are of nanometre scale dimensions. Unlike ferritin, there are no organised protein components associated with haemosiderin, although 17 kDa and 21 kDa peptides have been observed to be associated with some haemosiderins [3].

In both the cases of ferritin and haemosiderin, the structure of the iron oxyhydroxide component varies and may partly depend on the type of disease, the treatment administered and the organ in which it is deposited [3–6]. The iron oxyhydroxide particles found in ferritin have varying degrees of structural order as measured by

electron diffraction experiments. The well crystalline particles show five or six powder diffraction rings at positions consistent with those for the mineral ferrihydrite ($5Fe_2O_3 \cdot 9H_2O$) while poorly crystalline cores show only one or two rings. Cores of intermediate crystallinity are also found showing three or four rings. Haemosiderins show even more diversity in their iron oxyhydroxide structure. Not only do they encompass the range of degrees of crystallinity of ferrihydrite found in ferritin but also the forms based on the structure of the mineral goethite (α-FeOOH); forms that are non-crystalline are also found [4,7].

Understanding the relationship between the magnetic properties of ferritin (and haemosiderin) and the structure of its mineral core is of importance in the growing field of magnetic resonance imaging (MRI) of iron overloaded patients and the use of superparamagnetic iron oxides as contrast agents in MRI [8–14].

Interpretation of the magnetic properties of ferritin and haemosiderin in terms of the structure of the particles is complicated by the varying quantities of other trace anions, such as phosphate, in the particles. Phosphate tends to weaken the magnetic exchange interactions between iron atoms within a particle thus reducing the magnetic ordering temperature and apparent magnetic anisotropy energy barrier [15–18]. Recently, we have synthesised a series of ferritin cores with varying degrees of structural order but with no phosphate present [19]. We have also synthesized other ferritin cores with different levels of phosphate present. These synthetically reconstituted ferritins provide useful model compounds for the study of the relationship between structure and composition of the nanoscale mineral particles and their magnetic properties. The protein coat surrounding each particle prevents contact between particles and hence eliminates the complicating factors of inter-particle magnetic exchange interactions. It should be noted that this may not be the case for haemosiderin in vivo.

2. Materials and methods

2.1. Preparation of apoferritin

Apoferritin (protein without iron) was prepared by dialysing Cd-free horse spleen ferritin (Boehringer Mannheim) against 0.025 M 3-[*N*-morpholino]propanesulphonic acid (MOPS) (Sigma) containing 1% thioglycollic acid (Sigma) for 5 days or until the protein turned yellow. The protein was further dialysed against the same buffer solution containing 0.1% thioglycollic acid to further remove remaining iron from the protein, and finally against 0.1 M MOPS at pH 7.5. In some experiments, horse spleen apoferritin from Sigma was used without further treatment. The horse spleen apoferritins were filtered through 0.22 μm Millex®-GS sterile filters (Millipore) before use.

2.2. Reconstitution of ferritin with iron(III) oxyhydroxide

Ferritins were reconstituted at 4 °C and 55 °C by addition of $^{57}FeSO_4$ (0.5 mg $^{57}Fe\ ml^{-1}$) to 1 mg ml^{-1} horse spleen apoferritin in 0.1 M MOPS, pH 7.5 to give a

theoretical loading of 1500 Fe/apoferritin. The $^{57}Fe(II)$ solution was added slowly with constant swirling of the reaction mixture. Before reconstitution, all solutions and reagents were incubated for a few hours at the temperature at which the reconstitution was to be carried out. In an additional preparation for samples for extended X-ray absorption fine structure (EXAFS) studies, ferritins were reconstituted at 9 °C and 65 °C using $FeSO_4$ with natural isotope abundance.

2.3. Reconstitution of ferritin with iron(III) oxyhydroxide and phosphate

Ferritins were reconstituted at 25 °C to give an iron to apoferritin ratio of 1000 and cores with iron to phosphate ratios of approximately 8:1, 4:1, 2:1 and 1:1. On completion of reconstitution the final iron concentration was 1.05 mM and final phosphate concentrations were 0.13 mM (for 8:1), 0.26 mM (for 4:1), 0.52 mM (for 2:1) and 1.05 mM (for 1:1). Phosphate was provided as KH_2PO_4 and was added to each sample 30 min before addition of iron.

2.4. Analysis of iron and phosphate content of ferritins

Iron in apoferritin samples was determined by measuring the absorbance of the protein at 420 nm in a Hewlett Packard 8450 UV–VIS spectrophotometer. The quantity of iron and phosphate taken up by the ferritin during reconstitution was measured using inductively coupled plasma (ICP) spectrometry (Varian Liberty 200 ICP Emission Spectrometer).

2.5. Transmission electron microscopy and electron diffraction

Ferritins were diluted to approximately 1 mg ml^{-1}. One drop of each solution was then applied to a formvar coated 200 mesh copper grid. The drop was allowed to stand for about 10 min before excess liquid was drawn off using tissue paper. Electron micrographs and electron diffraction patterns were recorded using a JEOL 2000FX transmission electron microscope operating at 80 or 100 kV. The camera length of the microscope was calibrated with reference to the diffraction pattern from gold metal particles.

The diameters of ferritin cores were measured using vernier callipers on enlarged prints of electron micrographs. For cores with irregular shapes, measurements were made across the orientation that gave the largest dimension. A total of 112 cores were measured for the 4 °C ferritin, 143 cores for the 55 °C ferritin, 147 cores for the 7Fe:1P ferritin, and 147 cores for the 0.8Fe:1P ferritin.

2.6. EXAFS measurements

The EXAFS experiments were carried out at Beamline 7C of the Photon Factory, National Laboratory for High Energy Physics, Japan. The positron storage ring was operating at 2.5 GeV and had a beam lifetime of about 70 h. The average current during the measurements was 290 mA. The Fe K edge EXAFS measurements were performed on samples of ferritin reconstituted at 9 °C and 65 °C. The samples were

measured at room temperature and at 80 K. Samples with an absorption–thickness product of about 2 in the region just after the edge were mounted on adhesive tape. The spectra were measured in transmission, with the first ion chamber filled with N_2 gas and the second filled with a mixture of 15% Ar and 85% N_2. In order to suppress harmonics in the X-ray beam the Si(111) double-crystal monochromator was detuned from parallelism such that the output intensity decreased by about 50%.

The EXAFS was extracted from the measured X-ray absorption spectra by normalizing the spectra in the usual way. First, the pre-edge region was fitted to a Victoreen-type background: $A_0+A_3/E^3+A_4/E^4$ where E is the X-ray energy. The background was then extended into the edge and post-edge region and subtracted from the whole spectrum. After converting the spectrum above the energy E_{edge} of the absorption edge to the wavevector scale k according to $k=[(E-E_{edge})8\pi^2m_e/h^2]^{1/2}$, a second background was fitted to the EXAFS region of the spectrum. This background consisted of a smoothing spline $s(k)$ using cubic polynomials [20]. The EXAFS $\chi(k)$ was then obtained by forming the difference between the data $y(k)$ and the background and dividing by the height D of the absorption step at the edge: $\chi(k)=[y(k)-s(k)]/D$.

2.7. *Mössbauer spectroscopy*

Samples of ferritin solution were placed in 19 mm diameter holders and were frozen for Mössbauer spectroscopic measurements. Sample temperatures above 4.2 K were maintained with either (i) a closed-cycle helium gas expansion refrigerator (Air Products Expander Module DE 202) or (ii) a continuous-flow liquid helium cryostat (CF500, Oxford Instruments Ltd.). Temperature measurement was by means of a calibrated silicon diode thermometer for the DE 202 and a calibrated carbon glass thermometer with an ASL (Automatic Systems Ltd) resistance bridge for the CF500. Sample temperatures of 4.2 K were maintained with a liquid helium bath cryostat. Mössbauer spectra were recorded in transmission geometry using a ^{57}Co in rhodium source mounted on a constant acceleration drive. The source was driven with a double ramp waveform. Spectra were folded to eliminate the parabolic background due to the variation of solid angle between source and detector during the scans. The velocity scale was calibrated with reference to the spectrum of an iron metal foil at room temperature. Spectra were fitted with doublets of Lorentzian peaks and sextets generated from distributions of magnetic hyperfine field splittings using a sum of squares minimization routine. During the fitting procedure the areas and widths of each line of the doublet components were constrained to be equal. For the sextet components the area ratio of the outer to middle to inner pair of lines was constrained to be 3:2:1. The asymmetric line shapes of the sextet components were fitted with a computer program based on a model for goethite proposed by Bocquet et al. [21]. The program produced reasonable fits to the asymmetric line shapes of the spectra and was thus used to parameterize the data[3]. Values of the

[3] It should be noted that the parameters are not meant to be interpreted in terms of the original model proposed by Bocquet et al. for the Mössbauer spectra of goethite. The computer program was used simply because it gives a reproducible parameterized fit to the data when different starting parameters are used.

chemical isomer shift δ the quadrupole splitting ΔE_Q, magnetic hyperfine field splitting, B_{hf}, linewidth Γ and spectral area of each component were allowed to vary freely during the fitting procedure.

3. Results

3.1. Ferritin cores reconstituted at different temperatures

Transmission electron micrographs of horse spleen ferritin reconstituted at 4 °C and 55 °C are shown in Figs. 1(a) and 1(b). The mineral cores of ferritins reconstituted at 4 °C appear to be smaller compared with those reconstituted at 55 °C. Particle size distributions of the cores are shown in Figs. 2(a) and 2(b). The 4 °C sample has a mean core size of 4.74±0.10 nm while the 55 °C sample has a mean core size of 5.14±0.12 nm. A *t*-test performed on these measurements showed that there is a

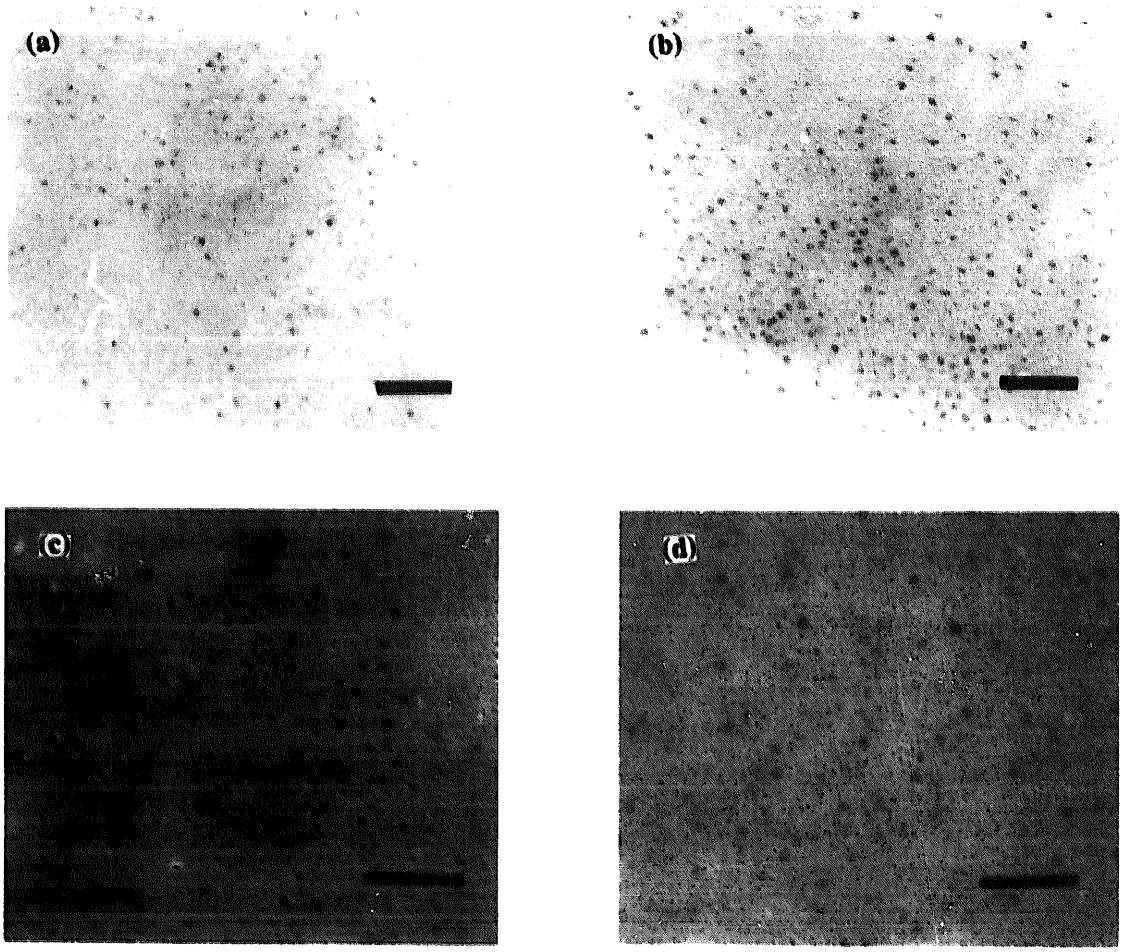

Fig. 1. Transmission electron micrographs of ferritins reconstituted with (a) 1500 Fe/apoferritin at 4 °C, (b) 1500 Fe/apoferritin at 55 °C, (c) 1000 Fe/apoferritin at 25 °C with Fe:P ratio of 7:1, and (d) 1000 Fe/apoferritin at 25 °C with Fe:P ratio of 0.8:1. Scale bar, 50 nm.

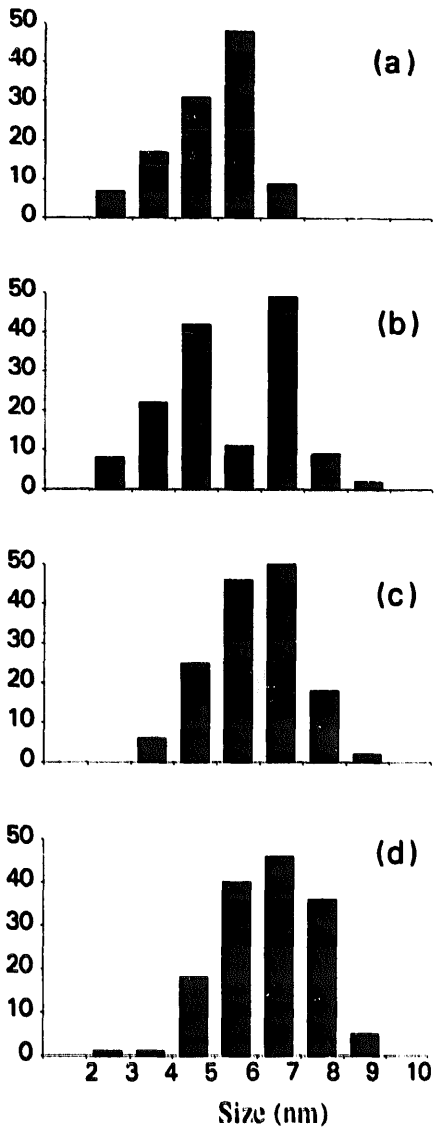

Fig. 2. Histograms illustrating the particle size distributions of the cores of ferritins reconstituted with (a) 1500 Fe/apoferritin at 4 °C, (b) 1500 Fe/apoferritin at 55 °C, (c) 1000 Fe/apoferritin at 25 °C with Fe:P ratio of 7:1, and (d) 1000 Fe/apoferritin at 25 °C with Fe:P ratio of 0.8:1.

significant difference in the particle sizes of ferritins reconstituted at the two temperatures ($p<0.01$).

Selected area electron diffraction patterns of ferritins reconstituted at 4 °C and 55 °C show powder diffraction rings at some of the positions that correspond to those of the mineral ferrihydrite ($5Fe_2O_3 \cdot 9H_2O$). Table 1 gives the *d*-spacings of the reconstituted ferritin cores as well as those of ferrihydrite. The 4 °C ferritins gave two diffuse powder diffraction lines while the 55 °C ferritins gave five diffraction lines. These results suggest that ferritin cores reconstituted at the higher temperature have a more ordered structure than those reconstituted at the lower temperature.

Normalized EXAFS spectra are shown in Fig. 3. In order to obtain qualitative

Table 1
Electron diffraction data (*d*-spacings) for ferrihydrite and reconstituted ferritins (nm)

Ferrihydrite[a]	4 °C ferritin	55 °C ferritin	7Fe:1P ferritin	0.8Fe:1P ferritin
0.250 s	—	0.264 s	—	—
0.221 ms	0.215 s	0.229 w	—	—
0.196 m	—	0.204 w	—	—
0.172 w	—	0.171 vw	—	—
0.151 m	0.158 w	0.154 s	0.153 vw	—
0.148 s	—	—	0.147 m	—

[a] Taken from Ref. [40]; s = strong; ms = medium strong; m = medium; w = weak; vw = very weak.

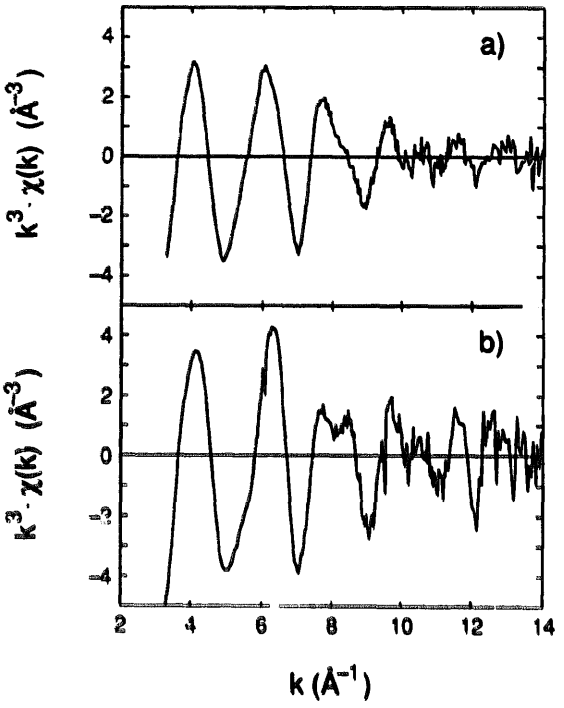

Fig. 3. k^3-weighted EXAFS spectra, measured at 80 K, of (a) ferritin reconstituted at 9 °C and (b) ferritin reconstituted at 65 °C.

information, the Fourier transform of the normalized EXAFS spectrum was calculated. This was done according to:

$$H(R) = (1/\sqrt{\pi}) \int_{-\infty}^{\infty} w(k)\chi(k)k^3 \exp(+i2kR)\mathrm{d}k$$

where $\chi(k)$ is the normalized EXAFS data and the term k^3 was introduced in order to compensate for the decrease of $\chi(k)$ with k. $w(k)$ is a Hamming window function [22] and was applied in order to suppress sidelobes in the Fourier transform. The magnitude of the Fourier transform, which was obtained directly from $H(R)$ and

which is related to the pair distribution function (PDF), exhibits two major peaks (Fig. 4). The first peak is due to the six nearest-neighbour oxygen atoms that surround the central iron atom and the second peak is assumed to be due to iron atoms. It can be seen from Fig. 4 that, with respect to the first peak, the second peak is larger in the sample of ferritin reconstituted at 65 °C. This is the case for all measurements and indicates that the 65 °C sample has either less disorder and/or more iron atoms in the second shell. If one assumes in a preliminary analysis that the peaks in Fig. 4 are related to Gaussian peaks in the PDF, then one finds that the corresponding s^2 values of the ferritin sample reconstituted at 65 °C are smaller than those for the 9 °C sample. Also, the number of iron atoms corresponding to the second peak is slightly larger for the 65 °C sample. Curve fitting directly to $\chi(k)$, employing two coordination shells, indicates that the 65 °C ferritin has an s^2 value for iron that is about 0.002 Å^2 smaller (at 300 K) than that of the 9 °C ferritin. At 80 K the s^2 value is 0.001 Å^2 smaller. The number of iron atoms corresponding to the second peak is approximately 3.5 for the 65 °C ferritin and about 3 for the 9 °C ferritin. This indicates that the sample of ferritin reconstituted at 65 °C has less disorder than the sample reconstituted at 9 °C. The preliminary analysis also indicates that for the 65 °C ferritin the radii of the coordination shells around the central iron atom are smaller by about 0.03 to 0.04 Å.

In our analysis only one oxygen coordination shell and one iron shell have been considered but the data indicate that more coordination shells are present. Both peaks seem to be due to two coordination shells each. The first peak may contain a second oxygen shell and the second peak may contain another iron or oxygen shell. Closely spaced coordination shells could explain the rather rapid decay of the EXAFS signal, shown in Fig. 3, which is not completely compensated, even by multiplying $\chi(k)$ by k^3. In early work on ferritin [23] it was concluded that there are only two coordination shells, namely oxygen and iron, as assumed in our preliminary analysis. However, a more recent study [24] found that the peaks are due to two coordination

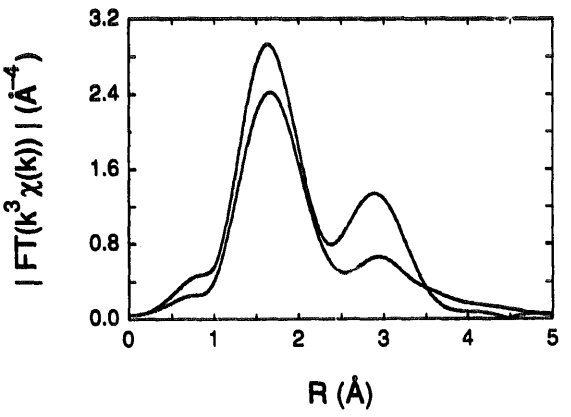

Fig. 4. Fourier transform magnitude of the k^3-weighted EXAFS at 80 K (Fig. 3) of ferritin reconstituted at 9 °C (lower curve) and at 65 °C (upper curve). The truncation interval for the Fourier transform extended from $k_{min} = 3.6$ Å^{-1} to $k_{max} = 11.3$ Å^{-1}. A Hamming window function was used.

shells each, which is closer to our interpretation. Indications for a phase transition, as postulated in [23], were not found.

An inspection of the Fe K absorption edges showed subtle differences between the edges corresponding to the ferritin samples reconstituted at 9 °C and 65 °C. This probably indicates that the immediate environment around the Fe atoms is slightly different for the two cases. However, for both samples the Fe K absorption edges occur at approximately 7120 eV. This value is 9 eV above the absorption edge position of Fe metal and suggests that only Fe(III) is present in our samples. No shoulder indicative of an admixture of Fe(II) could be detected in the absorption edge jumps.

Mössbauer spectra of ferritins reconstituted at 4 °C and 55 °C were recorded at 13.5 K and 4.2 K (Figs. 5 and 6). Mössbauer spectral parameters obtained from fits to the data are given in Table 2 and are all within the range for Fe(III). At 13.5 K, both spectra show a coexistence of a magnetic-hyperfine-field (B_{hf}) split sextet and a central component. The central component is almost extinguished at 4.2 K. The coexistence of the sextet component and the central component in the Mössbauer spectra, the disappearance of the sextet in the wings of the spectrum and increase in the central component as the temperature is raised are characteristics that indicate superparamagnetic behaviour in the ferritin cores [15].

The spectrum of the 4 °C ferritin at 13.5 K has a higher percentage area of the

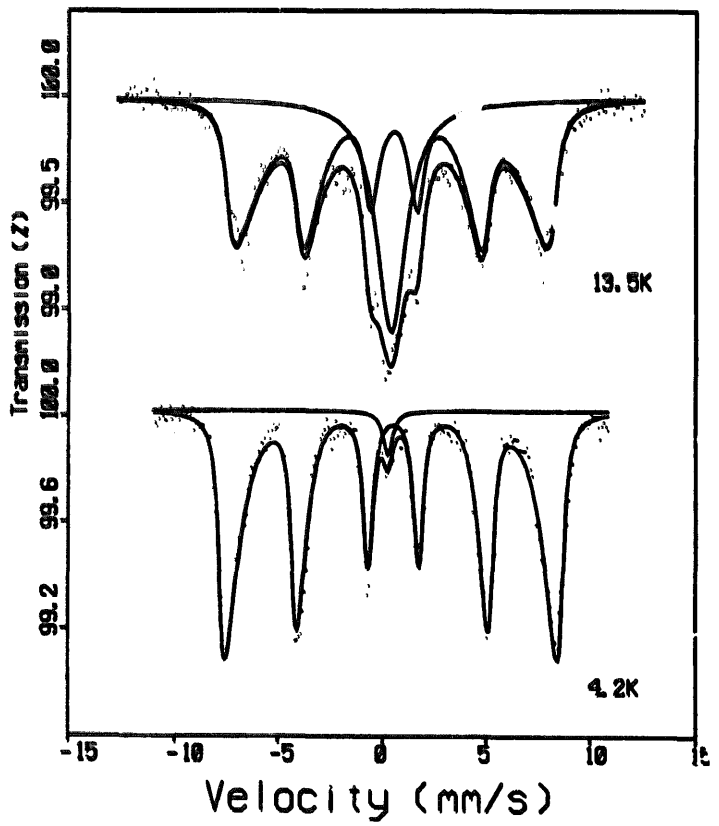

Fig. 5. Mössbauer spectra of ferritin (reconstituted with 1500 Fe/apoferritin at 4 °C) at 13.5 and 4.2 K.

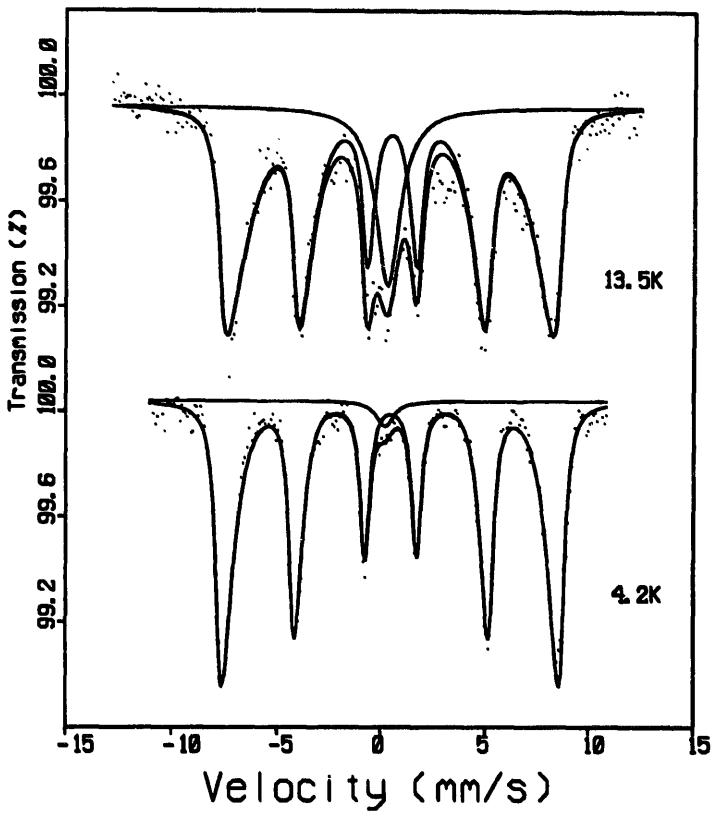

Fig. 6. Mössbauer spectra of ferritin (reconstituted with 1500 Fe/apoferritin at 55 °C) at 13.5 and 4.2 K.

central component than the 55 °C ferritin (Table 2). This indicates that the 4 °C sample has a lower magnetic anisotropy energy which suggests a lower degree of crystallinity and/or fewer iron atoms per core than the 55 °C ferritin.

In addition, the 55 °C ferritin has a larger B_{hf} splitting with more symmetric lineshapes than the 4 °C ferritin at both 13.5 K and 4.2 K (Table 2). The larger B_{hf} and less asymmetrically broadened lines of the 55 °C ferritin are consistent with the presence of a higher degree of structural order of the iron(III) oxyhydroxide cores which would give rise to stronger magnetic exchange interactions among the iron atoms.

3.2. *Ferritin cores reconstituted with different quantities of phosphate*

Horse spleen apoferritin samples were reconstituted with iron in the presence of different amounts of phosphate and were then dialysed to remove unbound iron and phosphate. ICP analyses of the four reconstituted ferritins gave Fe:P ratios of 7:1, 4:1, 1.5:1 and 0.8:1. The very low Fe:P ratios obtained for the latter two samples suggest that a reasonably large fraction of the phosphate is bound within the core structure rather than simply on the surface of the core.

Transmission electron micrographs of the 7Fe:1P and 0.8Fe:1P reconstituted ferritins are shown in Figs. 1(c) and 1(d). The core images of the 0.8Fe:1P ferritin

Table 2
Mössbauer spectral parameters of reconstituted ferritins derived from fits to the data

Sample	Temperature (K)	Doublet				Sextet				
		δ	ΔE_Q	Γ	%A	δ	ΔE_Q	B_{hf} (mean)	B_{hf} (max)	%A
4 °C ftn	13.5	0.40	—	—	15	0.45	−0.05	44.5	47.8	85
	4.2	0.23*	—	—	2*	0.46	−0.07	48.4	50.4	98
55 °C ftn	13.5	0.30	—	—	8	0.46	−0.09	46.8	49.5	92
	4.2	0.20*	—	—	1*	0.45	−0.04	49.2	50.7	99
7Fe:1P ftn	40	0.43	0.77	0.68	74	broad component				26
	28.9	0.45	0.66	0.75	23	0.40	−0.20	37.9	48.6	77
	4.2	0.37*	—	—	1	0.45	−0.02	48.2	50.0	99
0.8Fe:1P ftn	40	0.46	0.82	0.57	100	—	—	—	—	—
	15.7	0.48	0.79	0 50	46	0.50	−0.22	45.6	50.9	54
	4.2	0.32*	—	—	3*	0.46	−0.05	45.1	49.3	97

δ is the chemical isomer shift (mm s^{-1}), ΔE_Q is the quadrupole splitting of the doublet or the quadrupole perturbation on the magnetic hyperfine field splitting (mm s^{-1}), Γ is the full width at half height of the peaks in the doublet (mm s^{-1}), %A is the percentage spectral area of each component, B_{hf}(mean) is the mean magnetic hyperfine field splitting (T) and B_{hf}(max) is the maximum value of the magnetic hyperfine field distribution (T). Approximate errors for these parameters are ± 0.02 mm s^{-1} (δ), ± 0.03 mm s^{-1} (ΔE_Q), ± 0.02 mm s^{-1} (Γ), ± 1 (%A), ± 0.5 T (B_{hf}(mean)), ± 0.5 T (B_{hf}(max)). *indicates a somewhat larger error due to the low intensity of the spectral component and high degree of overlap with major component.

appear to have less contrast in general than those for the 7Fe:1P ferritin, suggesting that the electron density of the cores is less for the 0.8Fe:1P sample. Particle size distributions measured from the core images are shown in Figs. 2(c) and 2(d). The 7Fe:1P ferritin has a mean core size of 5.89 ± 0.08 nm while the 0.8Fe:1P ferritin has a larger mean core size of 6.28 ± 0.09 nm. A t-test performed on these measurements showed that there is a significant difference between these two mean particle sizes ($p < 0.01$).

Selected area electron diffraction patterns of the ferritins reconstituted with phosphate gave one medium intensity and one very weak powder diffraction ring in positions corresponding to two of those in the ferrihydrite pattern for the 7Fe:1P ferritin (Table 1). However, no diffraction pattern was observed for the 0.8Fe:1P ferritin, indicating a non-crystalline structure.

Mössbauer spectra of the reconstituted ferritins with Fe:P ratios of 7:1 and 0.8:1 are shown in Figs. 7 and 8. Mössbauer spectral parameters obtained from fits to the data are given in Table 2 and are all within the range for iron(III).

At 4.2 K the 7Fe:1P ferritin gives a Mössbauer spectrum that consists mainly of a sextet of broad peaks with a mean B_{hf} splitting of 48.2 T. There is a small (approximately 1%) central component whose features are difficult to determine

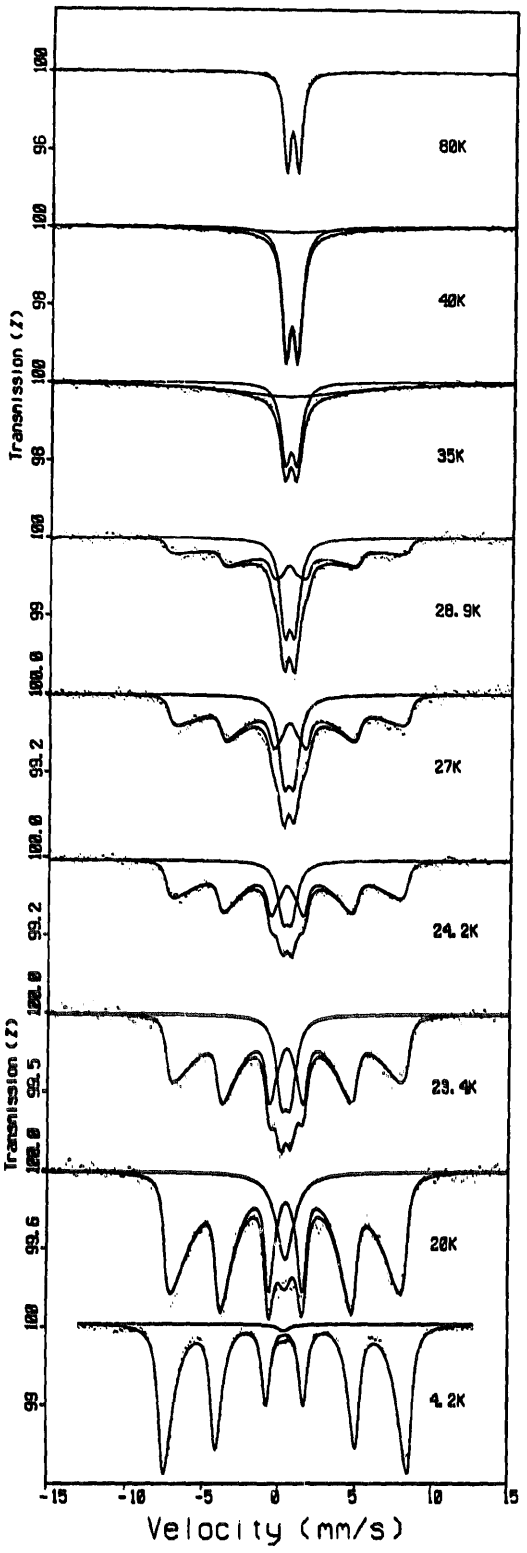

Fig. 7. Mössbauer spectra of ferritin (reconstituted with 1000 Fe/apoferritin at 25 °C with 7Fe:1P) over a range of temperatures from 4.2 to 80 K.

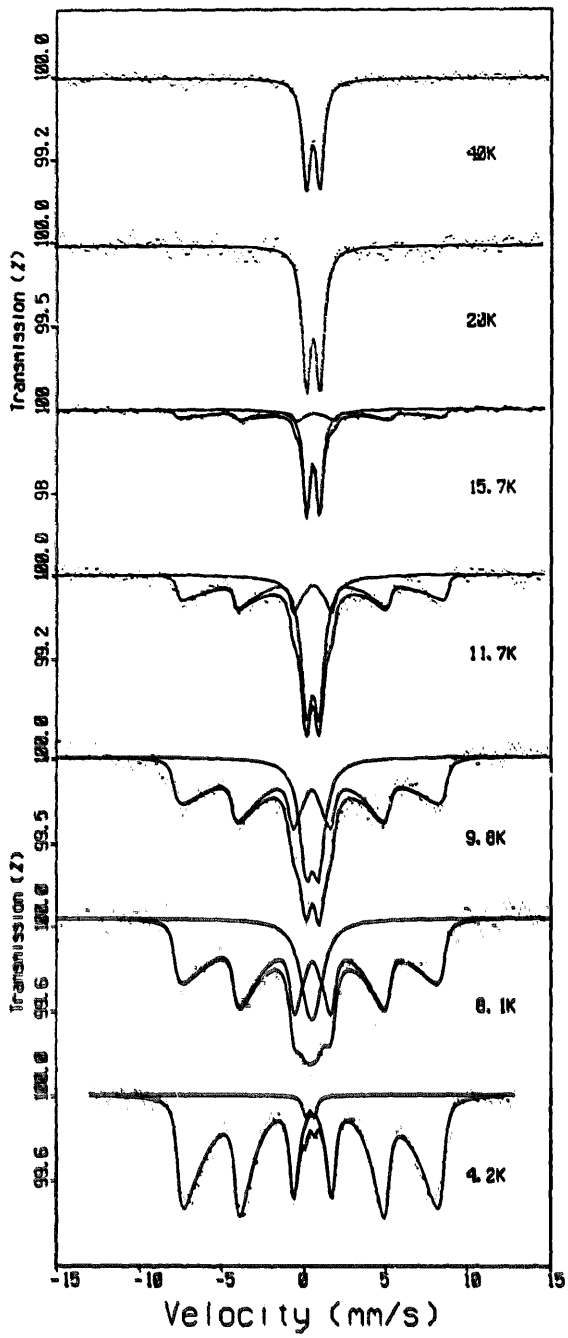

Fig. 8. Mössbauer spectra of ferritin (reconstituted with 1000 Fe/apoferritin at 25 °C with 0.8Fe:1P) over a range of temperatures from 4.2 to 40 K.

because of its low intensity. As the temperature is raised above 4.2 K the peaks of the sextet component broaden asymmetrically and their intensity decreases while the intensity of the central component increases. At 27 K and above the central component can be resolved into a doublet of peaks. The coexistence of the central doublet component with the B_{hf} split sextet and its growth and concomitant decrease of the

sextet component with increasing temperature are characteristics of superparamagnetic materials. The doublet component corresponds to iron atoms in particles that have superparamagnetic relaxation rates greater than the Larmor precession frequency of the ^{57}Fe nucleus in B_{hf} (approximately 10^8 s^{-1}) while the sextet component corresponds to iron atoms in particles with superparamagnetic relaxation rates less than this frequency. At approximately 33 K the doublet makes up 50% of the spectral area. The mean B_{hf} splitting decreases from 48.2 T at 4.2 K to 37.9 T at 28.9 K. This is mainly due to the asymmetric broadening of the peaks (i.e. the distribution of B_{hf} covers lower values). The maximum value in the B_{hf} distribution drops slightly from 50.0 T at 4.2 K to 48.6 T at 28.9 K. At 35 K the B_{hf} distribution is very broad and difficult to fit with a meaningful distribution. The B_{hf}-split component is almost extinguished by 40 K.

Qualitatively, the Mössbauer spectral behaviour of the 0.8Fe:1P ferritin is similar to that of the 7Fe:1P ferritin. However, there are significant quantitative differences. At 4.2 K the mean B_{hf} is somewhat smaller than that for the 7Fe:1P ferritin (45.1 T cf. 50.0 T) and the peaks of the sextet are more asymmetrically broadened. The decrease in the intensity of the sextet component as temperature is increased is more rapid, the central doublet making up 50% of the spectral area by approximately 17 K (cf. approximately 33 K for 7Fe:1P ferritin). By 20 K the B_{hf} split component is completely extinguished. The mean B_{hf} splitting varies very little between 4.2 and 15.7 K.

4. Discussion

The transmission electron microscopy, electron diffraction, EXAFS and Mössbauer spectroscopy data indicate that reconstitution of horse spleen apoferritin with iron at different temperatures results in cores with different particle size distributions and degrees of structural order. The structure of the cores appears to be based on that of the mineral ferrihydrite. The cores are larger and more ordered when formed at 55 °C compared with those formed at 4 °C. This result can be understood in several ways [19].

From a crystal growth point of view, the different core structures can be explained in terms of diffusion of ions across the growing core surface. New ions arriving at the core surface would have many different initial binding sites with a variety of potential energies. Diffusion of the ions across the surface of the core will be enhanced at higher temperatures where thermal activation enables the activation energy barriers separating the different surface locations to be overcome. In this way, at higher temperatures, ions will be more likely to find sites of lowest energy before the next layer of ions is deposited which would then trap them in whichever site they happen to be in at that time. Thus a more regular arrangement of ions is built up at the higher temperatures.

Another factor that may influence core growth is any change in conformation of the protein shell at different temperatures. Conformational changes may affect the channels that facilitate the transport of ions into and out from the central cavity,

thus hindering or aiding the rate of diffusion of ions to the core. Active binding sites on the inner surface of the protein could also be altered, thus affecting the nucleation rate. Further, the cavity size may also change, thus changing the maximum core size attainable. The temperature dependence of the conformation of ferritin, however, has not yet been reported.

The slightly lower value of the B_{hf}-splitting in the Mössbauer spectrum of the 4 °C ferritin at 4.2 K compared with that for the 55 °C ferritin indicates slightly weaker magnetic exchange interactions between the iron atoms within a ferritin core. This is probably due to either larger iron–iron distances within the cores of the 4 °C ferritin or to a reduced number of iron neighbours for each iron atom (i.e. an increased number of vacancies) as indicated by the EXAFS analysis. Similar reductions in magnetic hyperfine field splittings at 4.2 K have been seen in the poorly crystalline cores of molluscan ferritins compared with those for well crystalline mammalian ferritins [15,17,25]. The larger fraction of iron atoms in particles with unblocked superparamagnetic moments at 13.5 K in the 4 °C ferritin compared with the 55 °C ferritin indicates that the magnetic anisotropy energy barriers are smaller for the 4 °C ferritin. Again, this is similar to the results found for the poorly ordered molluscan ferritins when compared with well ordered mammalian ferritins. The smaller magnetic anisotropy energy barriers for the more poorly ordered core structures are expected since the total magnetic anisotropy field for a particle is the vectorial sum of the magnetic anisotropy fields of the individual iron atoms within the particle. For more disordered structures, the individual fields will add less coherently and therefore the energy barrier height will not be as large.

Reconstitution of ferritin with phosphate incorporated into the core structure influences both the structure and magnetic properties of the cores. The transmission electron microscopy and electron diffraction data indicate that the ferritins reconstituted with 1000 Fe/apoferritin in the presence of phosphate at 25 °C have significantly larger but less crystalline cores than ferritins reconstituted with 1500 Fe/apoferritin in the absence of phosphate at 4 and 55 °C. The suppression of structural order within the iron-containing mineral core of ferritin when phosphate is incorporated into the structure is in keeping with all previous observations of iron biominerals that contain high levels of phosphate. Some examples of these materials are: the mineral cores of the bacterioferritins from *Pseudomonas aeruginosa* [26] and *Azotobacter vinelandii* [27]; components of the sternal shields of the annelid, *Sternaspis scutulata* [28]; subunits of the mature teeth of the chiton, *Cryptochiton stelleri* [28]; the inner subunits of the gizzard plates of the gastropod, *Scaphander cylindrellus* [28]; the dermal granules of the holothuroid, *Molpadia intermedia* [28,29]; and abdominal particles in the honey bee, *Apis mellifera* [30,31]. These materials give no X-ray diffraction and/or electron diffraction patterns and contain high levels of phosphate. No biological iron minerals with iron to phosphate ratios of between 1:1 and 2:1 have yet been found to be crystalline. This suggests that the presence of high levels of phosphate is associated with non-crystallinity in iron biominerals [15,32].

The larger particle size of the ferritin cores reconstituted with phosphate indicates that either fewer cores have been created per apoferritin when phosphate is present

or, assuming that all ferritin molecules contain a core, that the cores are less dense when phosphate is incorporated. The contrast in the transmission electron micrographs of the phosphate loaded ferritins appeared less than that for the phosphate free ferritins, the 0.8Fe:1P ferritin having the least contrast in the core images, suggesting that the phosphate loaded cores may well be less dense. This can be understood in terms of the fact that the PO_4^{3-} ions have much larger ionic radii than the OH^- ions. In addition, the higher degree of disorder within the phosphate loaded cores would be expected to reduce the density further. These observations are in keeping with those on native ferritins from mammalian and bacterial sources. Mammalian ferritins tend to have Fe:P ratios of about 8:1 with approximately 3000 Fe/ferritin while bacterial ferritins tend to have Fe:P ratios of about 1:1 with only 1000 Fe/ferritin [15]. Similar core sizes are found for both categories indicating a less dense core structure for the bacterial ferritins.

At 4.2 K the 7Fe:1P ferritin shows a mean B_{hf}-splitting in the Mössbauer spectrum similar to that of the 4 °C ferritin. However, the 0.8Fe:1P ferritin shows a mean B_{hf}-splitting at 4.2 K that is noticeably smaller, indicating a substantial decrease in the strength of the magnetic exchange interactions between the iron atoms within the ferritin cores. This effect of the presence of large amounts of phosphate within ferritin cores has been observed previously in several bacterial ferritins [17,18,33,34]. Since the presence of high levels of phosphate within ferritin cores always appears to disrupt the regularity of the core structure [15], the reduction in the strength of the magnetic exchange interactions may be partly due to the increased disorder as discussed for the 4 °C ferritin. However, the phosphate ion itself may play a role in reducing the magnetic exchange interaction strength. The PO_4^{3-} ion being much larger than the OH^- ion will also tend to push the iron atoms further apart. Magnetic studies on model Fe–P–O compounds show that there is a drop of an order of magnitude in the magnetic ordering temperatures of the materials when the Fe:P ratios fall below 2:1. Fe_3PO_7, Fe_2PO_5 and $Fe_9(PO_4)O_8$ have magnetic ordering temperatures of 160 K, 250 K and 217 K respectively [35–37], while Fe–P–O compounds with Fe:P less than 2:1 such as $FePO_4$, $Fe_7(PO_4)_6$, $Fe_2P_2O_7$, $Fe_2P_4O_{12}$ and a glassy compound of approximate composition $Fe_3P_5O_{17}$ have magnetic ordering temperatures of 23.8 K, 10 K, 21 K, 18.5 K and 7 K respectively [38,39].

The mean superparamagnetic blocking temperatures for the 7Fe:1P and 0.8Fe:1P ferritins are approximately 33 K and 17 K respectively. Thus the magnetic anisotropy energy barriers of the cores are lowered by the increased phosphate content. This is consistent with the higher degree of disorder present in the 0.8Fe:1P ferritin cores. However, the fact that magnetic hyperfine field splitting is observed in the 0.8Fe:1P ferritin indicates that the magnetic exchange interactions may not be as weak as those observed in the high-phosphate-containing bacterial ferritin cores studied previously [11,18,33,34]. This may be an indication that some of the phosphate is bound to the protein or to the surface of the core rather than within the core structure, making the Fe:P ratio within the core structure somewhat higher than 0.8:1. Nevertheless, such a low Fe:P ratio for the ferritin as a whole must indicate that a reasonably large fraction of the phosphate is bound within the core structure.

In conclusion, it has been shown that ferritin can be reconstituted under different

controlled conditions to provide cores with tailored structural and compositional properties. These reconstituted ferritins can be used as model materials for probing the relationship between the magnetic properties of nanoscale iron biomineral deposits and their structure and composition. Information gained from these types of study will be used in the interpretation of magnetic measurements on iron biomineral deposits such as ferritin and haemosiderin in pathological tissue samples from iron-overload diseases. Magnetic measurements are of importance because of the specificity of the iron to the magnetic properties of the tissue, thus allowing measurements on bulk unfractionated tissue samples to be interpreted in terms of the iron biomineral deposits present. Ultimately, the information will help in the interpretation of MRI scans of iron-loaded patients.

Acknowledgements

This work was supported by the National Health and Medical Research Council (Australia). For part of the work TS thanks the Cooley's Anemia Foundation, New York for a Fellowship. The EXAFS measurements were made with the financial support of the Australian National Beamline Facility and the cooperation of Professor M. Nomura.

References

[1] P.M. Harrison, P.J. Artymiuk, G.C. Ford, D.M. Lawson, J.M.A. Smith, A. Treffry and J.L. White, in S. Mann, J. Webb and R.J.P. Williams (eds.), Biomineralization: Chemical and Biochemical Perspectives, VCH, Weinheim, 1989, p. 257.
[2] A. Jacobs, in A. Jacobs and M. Worwood (eds.), Iron in Biochemistry and Medicine 2, Academic Press, London, 1980, p. 427.
[3] R.J. Ward, M. Ramsey, D.P.E. Dickson, C. Hunt, T. Douglas, S. Mann, F. Aouad, T.J. Peters and R.R. Chrichton, Eur. J. Biochem., 225 (1994) 187.
[4] S. Mann, V.J. Wade, D.P.E. Dickson, N.M.K. Reid, R.J. Ward, M. O'Connell and T.J. Peters, FEBS Lett., 234 (1988) 69.
[5] T.G. St. Pierre, K.C. Tran, J. Webb, D.J. Macey, B.R. Heywood, N.H. Sparks, V.J. Wade, S. Mann and P. Pootrakul, Biol. Met., 4 (1991) 162.
[6] T.G. St. Pierre, K.C. Tran, J. Webb, D.J. Macey and P. Pootrakul, in S. Suga and H. Nakahara (eds.), Mechanisms and Phylogeny of Mineralization in Biological Systems, Springer-Verlag, Tokyo, 1991, p. 291.
[7] V.F. Wohler, Acta Haematol., 23 (1960) 342.
[8] E. Rocchi, M. Cassanelli, A. Borghi, F. Paolillo, M. Pradelli, G. Casalgrandi, A. Burani and E. Gallo, Hepat., 17 (1993) 997.
[9] G. Frija, O. Clement and E. de Kerviler, Investigative Radiology, 29 (Suppl. 2) (1994) S75.
[10] J.W.M. Bulte, T. Douglas, S. Mann, R.B. Frankel, B.M. Moskowitz, R.A. Brooks, C.D. Baumgarner, J. Vymazal and J.A. Frank, Invest. Radiol., 29 (Suppl. 2) (1994) S214.
[11] H. Trillaud, P. Degreze, C. Combe, J. Palussiere, C. Chambon and N. Grenier, Invest. Radiol., 29 (1994) 540.
[12] S. Bondestam, A. Lamminen, V.J. Anttila, T. Ruutu and P. Ruutu, Br. J. Radiol., 67 (1994) 339.
[13] P.D. Jensen, F.T. Jensen, T. Christensen and J. Ellegaard, Br. J. Haematol., 87 (1994) 171.

[14] S.H. Koenig, in R.B. Frankel and R.P. Blakemore (eds.), Iron Biominerals, Plenum, New York, 1990, p. 359.
[15] T.G. St. Pierre, J. Webb and S. Mann, in S. Mann, J. Webb and R.J.P. Williams (eds.), Biomineralization: Chemical and Biochemical Perspectives, VCH, Weinheim, 1989, p. 295.
[16] T.G. St. Pierre, D.P.E. Dickson, J. Webb, K.S. Kim, D.J. Macey and S. Mann, Hyper. Interact., 29 (1986) 1427.
[17] T.G. St. Pierre, S.H. Bell, D.P.E. Dickson, S. Mann, J. Webb, G.R. Moore and R.J.P. Williams, Biochim. Biophys. Acta., 870 (1986) 127.
[18] E.R. Bauminger, S.G. Cohen, D.P.E. Dickson, A. Levy, S. Ofer and J. Yariv, Biochim. Biophys. Acta., 623 (1980) 237.
[19] P. Chan, W. Chua-anusorn, M. Nesterova, P. Sipos, T.G. St. Pierre, J. Ward and J. Webb, Aust. J. Chem., 48 (1995) 783.
[20] K.R. Bauchspiess, Physica B, 208–209 (1995) 183.
[21] S. Bocquet, R.J. Pollard and J.D. Cashion, Phys. Rev. B, 46 (1992) 11657.
[22] F.J. Harris, Proc. IEEE, 66 (1978) 51.
[23] S.M. Heald, E.A. Stern, B. Bunker, E.M. Holt and S.L. Holt, J. Am. Chem. Soc., 101 (1979) 67.
[24] P. Mackle, C.D. Garner, R.J. Ward and T.J. Peters, Biochim. Biophys. Acta., 1115 (1991) 145.
[25] T.G. St.Pierre, K.S. Kim, J. Webb, S. Mann and D.P.E. Dickson, Inorg. Chem., 29 (1990) 1870.
[26] S. Mann, J.V. Bannister and R.J.P. Williams, J. Mol. Biol., 188 (1986) 225.
[27] S. Mann, J.M. Williams, A. Treffry and P.M. Harrison, J. Mol. Biol., 198 (1987) 405.
[28] H.A. Lowenstam, Chem. Geol., 9 (1972) 153.
[29] S. Ofer, G.C. Papaefthymiou, R.B. Frankel and H.A. Lowenstam, Biochim. Biophys. Acta., 676 (1981) 199.
[30] D.A. Kuterbach, B. Walcott, R.J. Reeder and R.B. Frankel, Science, 218 (1982) 695.
[31] D.A. Kuterbach and B. Walcott, J. Exp. Biol., 126 (1986) 375.
[32] S. Mann, in R.E. Crick (ed.), Origin, Evolution, and Modern Aspects of Biomineralization in Plants and Animals, Plenum, New York, 1989, p. 273.
[33] P.L. Ringeling, S.L. Davy, F.A. Monkara, C. Hunt, D.P.E. Dickson, A.G. McEwan and G.R. Moore, Eur. J. Biochem., 223 (1994) 847.
[34] H. Winkler, W. Meyer, A.X. Trautwein and B.F. Matzanke, Hyper. Interact., 91 (1994) 841.
[35] A. Modaressi, A. Courtois, R. Gerardin, B. Malaman and C. Gleitzer, J. Solid State Chem., 40 (1981) 301.
[36] A. Modaressi, A. Courtois, R. Gerardin, B. Malaman and C. Gleitzer, J. Solid State Chem., 47 (1983) 245.
[37] G. Venturini, A. Courtois, J. Steinmetz, R. Geradin and C. Gleitzer, J. Solid State Chem., 53 (1984) 1.
[38] G.J. Long, A.K. Cheetham and P.D. Battle, Inorg. Chem., 22 (1983) 3012.
[39] T. Ericsson, A.G. Nord, M.M.O. Ahmed, A. Gismelseed and F. Khangi, Hyper. Interact., 57 (1990) 2179.
[40] P. Bayliss, L.G. Berry, M.E. Mrose and D.K. Smith, Mineral powder diffraction file data book, Joint Committee on Powder Diffraction Standards, International Centre for Diffraction Data, Swarthmore, 1980.